frontiers | Frontiers in Astronomy and Space Sciences

TYPE Original Research
PUBLISHED 06 February 2025
DOI 10.3389/fspas.2024.1490090

OPEN ACCESS

EDITED BY
Lyle Whyte,
McGill University, Canada

REVIEWED BY
José Manuel Martínez Lozano,
Autonomous University of Madrid, Spain
María Colín-García,
National Autonomous University of Mexico, Mexico

*CORRESPONDENCE
Max Riekeles,
riekeles@tu-berlin.de

RECEIVED 02 September 2024
ACCEPTED 09 December 2024
PUBLISHED 06 February 2025

CITATION
Riekeles M, Bruder V, Adams N, Santos B and Schulze-Makuch D (2025) Application of chemotactic behavior for life detection. *Front. Astron. Space Sci.* 11:1490090. doi: 10.3389/fspas.2024.1490090

Application of chemotactic behavior for life detection

Max Riekeles[1]*, Vincent Bruder[1,2], Nicholas Adams[1], Berke Santos[1,3] and Dirk Schulze-Makuch[1,4,5]

[1]Astrobiology Group, Center of Astronomy and Astrophysics, Technical University Berlin, Berlin, Germany, [2]Department of Biology, Humboldt-Universität zu Berlin, Berlin, Germany, [3]Instituto Superior Técnico, Universidade de Lisboa, Lisboa, Portugal, [4]German Research Centre for Geosciences (GFZ), Section Geomicrobiology, Potsdam, Germany, [5]Department of Plankton and Microbial Ecology, Leibniz Institute of Freshwater Ecology and Inland Fisheries, Stechlin, Germany

One excellent biosignature for the present detection of microbial life on Earth is motility, leading to its growing interest within the astrobiological community as an observable attribute that, if detected during future *in situ* space missions, could point towards the existence of life on Mars or other celestial bodies. Microbial motility can be induced by various stimulants, including certain chemicals called chemoeffectors, leading to subsequent chemotaxis. Following this concept, this work examines the chemotactic affinities of the bacteria *Bacillus subtilis* and *Pseudoalteromonas haloplanktis* as well as the archaeon *Haloferax volcanii* for L-serine, which has been previously demonstrated to have a high chemoeffective potency across a wide range of species from all domains of life on Earth. Methodologically, we introduce here a novel approach for utilizing µ-slides that diverges from the more traditional long-term chemotactic assay in favor of a shorter time frame assay that only requires a simple blob detection algorithm for microbial detection. Given the technical, computational, and time constraints necessary for an *in-situ* life detection mission, this simplified approach could be a cost and resource-effective way to probe for potential chemotactic-responsive life. Overall, the results indicated that each of the three organisms showed chemotactic behavior toward L-serine, which, to our knowledge, is the first time that an L-serine-induced chemotactic response has been detected for *H. volcanii*.

KEYWORDS

chemotaxis, microbial motility, life detection, prokaryotes, microscopy, biosignature

1 Introduction

Even when using advanced electron microscopical techniques, it is not always possible to clearly distinguish primitive life forms like bacteria and archaea from nonliving mineral particles (Thomas-Keprta et al., 2002). In the context of detecting life on Mars and other foreign worlds, the degree of difficulty is exacerbated by device vibration throughout the voyage, temperature sensitivity, and, amongst other challenges, a higher necessary threshold of operator expertise. Nevertheless, every planetary mission has used optical equipment for imaging, but the focus has primarily been on geological studies rather than the direct observation of potential microorganisms (Nadeau et al., 2018). To date, no direct microscopic observations have been made on Mars with sufficient resolution to detect bacteria

or other microscopic life forms (Nadeau et al., 2016). There is, therefore, a need for the development of life-detection instruments, which may involve machine learning algorithms, that can be employed with minimal resources yet still retain the capacity to sufficiently detect microbial life and differentiate it from the surrounding environment (Riekeles et al., 2021).

Microbial motility, the directed motion of microbes under their own propulsion, can be clearly distinguished from random Brownian movement by microscopic techniques and is, therefore, a prominent biosignature of life (Thomas-Keprta et al., 2002; Lindensmith et al., 2016; Nadeau et al., 2016; Nadeau et al., 2018; Riekeles et al., 2021; Riekeles et al., 2024b). Given that it has evolved independently multiple times on Earth (Miyata et al., 2020), motility might also be a fundamental trait of extraterrestrial life that can be exploited for its detection in a resource-depleted setting (Neveu et al., 2018). Motility, a characteristic present across all three domains of life—bacteria, archaea, and eukaryotes—can be derived via several molecular mechanisms in response to various environmental cues, such as avoiding harmful substances or locating new resources and nutrients (Allen, 1981). The run-and-tumble method is one such motility pattern in several prokaryotes (Madigan et al., 2018, pp. 92–100). The clockwise or counterclockwise rotation of filamentous appendages, which are capable of rotating at speeds of up to 1,000 revolutions per second, allows bacteria (Madigan et al., 2018, pp. 92–100) to alternate between swimming phases (i.e., runs) and tumbling phases (i.e., changes in direction). The swimming phase propels the cell forward at speeds up to 60 cell lengths per second, whereas the tumbling phase involves reorientations of swimming direction. The Mot proteins (MotA and MotB) located in the cytoplasmic membrane selectively conduct protons, thereby providing a proton motive force (PMF) that can serve as the necessary energy source for rotation (Bardy et al., 2003).

Other common bacterial motility forms include twitching motility, sliding motility, and flagellar propulsion. Twitching motility involves a cyclic pulling mechanism via the extension, fastening, and retraction of cellular attachments referred to as type IV pili (Merz et al., 2000; Skerker and Berg, 2001; Mattick, 2002; Craig et al., 2019). Sliding motility, instead, relies on the expansive forces of cell growth within a colony (Hölscher and Kovács, 2017). Alternatively, spirochetes have evolved to utilize flagella stemming from the periplasmic space (between their outer membrane and cell wall) at opposing ends of the cell. The coordinated rotation of these flagella provides movement when rotating symmetrically and restricts movement when rotating asymmetrically (Bardy et al., 2003).

Following the concept of the ubiquitous nature of motility, many archaea also use an appendage that is functionally similar but structurally distinct from the bacterial flagellum (Albers and Jarrell, 2018). The archaellum consists of a helical filament attached to a membrane-embedded motor complex. This filament is composed of proteins called archaellins, which are synthesized as pre-proteins in a manner similar to that of the type IV pili in bacteria (Jarrell et al., 2021). Unlike bacterial flagella, which make use of electrochemical gradients, the archaellum presumably uses ATP as its energy source (Nuno de Sousa Machado et al., 2022). Both the archaellum's preserved ability to rotate clockwise and counterclockwise and the large percentage of amino acid sequence overlap with flagellin, a key protein in the filament region of bacterial flagella, suggest that flagellar-like motility has deep evolutionary roots in the history of life. Furthermore, archaea appear to have acquired their chemosensory systems from bacteria and, subsequently, have successfully integrated these systems with the archaellum (Li et al., 2019). Despite these seemingly ancient similarities, structural comparison of the flagellar proteins from the archaeal archaellum and bacterial flagellum imply that flagellar motility evolved independently in these two groups, likely diverging over 3.5 billion years ago (Madigan et al., 2018).

There is a lack of consensus regarding the overall percentage of (known) motile prokaryotes, partially due to many studies focusing solely on using the genome to predict structure and function rather than making direct cellular observations. In 1996, approximately 80% of the bacteria described were motile by means of flagella (Aizawa, 1996). Utilizing more recent data from a BacDive database sample of 14,309 different bacterial strains, it was determined that 40% were motile (Reimer et al., 2022). The website is available at https://bacdive.dsmz.de/advsearch (accessed on 27 November 2024). Overall, the proportion of motile bacteria can vary widely in natural environments at any given sampling time, with reports indicating a range between 5% and 80% (Grossart et al., 2001; Fenchel and Thar, 2004). For example, a study on bacterial swimming behavior in the ocean near the Scripps pier in San Diego demonstrated that motility can vary seasonally (Soutourina et al., 2001).

Light stimuli (phototaxis), orientation in magnetic fields (magnetotaxis), and movement in response to chemical gradients, known as chemotaxis—the primary focus of this study—are among the most common stimulants of microbial motility. Numerous studies have demonstrated that bacteria predominantly utilize chemotaxis to migrate toward environmental conditions that optimize their growth, such as being attracted to amino acids and sugars (Colin et al., 2021). In certain bacterial species, the most potent chemoattractants align with the molecules that are preferentially consumed by the cells, as exemplified by *Escherichia coli's* response to specific L-amino acids (Yang et al., 2015; Colin et al., 2021). However, this strict correlation between the magnitude of chemotaxis and the direct metabolic or physiological advantages conferred by the chemoattractant does not always hold true in other bacterial species (Colin et al., 2021). For instance, the chemotactic system in *B. subtilis,* which was determined to have a heightened sensitivity to environmental cues (Yang et al., 2015), was found to be attracted to ethanol despite it not being a direct metabolic substrate nor providing seemingly any physiological benefit (Tohidifar et al., 2020). The authors proposed that ethanol conferred an indirect benefit to *Bacillus subtilis*, which could use the molecule to locate and prey on ethanol-fermenting microorganisms (Tohidifar et al., 2020). Rather than the chemoattractant leading directly to a beneficial metabolic or physiological source, this suggests a multistep process where bacteria utilize chemoattractants to locate particular environments that are more likely to contain their preferred nutrient sources (Colin et al., 2021).

Amino acids, particularly proteinogenic amino acids, have long been recognized as potent chemoattractants, presumably due to their essential role in biological processes (Mesibov and Adler, 1972; Vuppula et al., 2010). Some of the oldest and most critical biochemical pathways, such as carbon fixation methods, have

evolved around the need to synthesize such key amino acids (Braakman and Smith, 2012). Correspondingly, the high degree of chemotactic sensitivity for these molecules is best exemplified in some organisms by an abundance of proteinogenic amino acid receptors in their membranes. One such proteinogenic amino acid, L-serine, has been determined to be among the most potent chemoattractants for *B. subtilis* and various other microbes (Ordal and Gibson, 1977). This finding may stem from the fact that L-serine is particularly unique due to its hydroxyl group, which is only found in two proteinogenic amino acids and is a common site for regulatory phosphorylation and dephosphorylation by protein kinases and phosphatases, respectively (Oxenrider and Kennelly, 1993). Concerning its astrobiological relevance, L-serine has been found has been found in a meteorite and in the 162173 Ryugu asteroid, indicating its presence even before the formation of our Solar System (Koga and Naraoka, 2017; Naraoka et al., 2023). Given that early Earth and Mars were bombarded by carbonaceous asteroids, L-serine likely exists on Mars (Pizzarello and Shock, 2010; Zhu et al., 2022). If life developed on Mars with a similar biochemistry to known life on Earth, it seems plausible that L-serine could also be a potent chemoattractant for hypothetical Martian microbes. In the field of astrobiology, chemotaxis has been discussed and investigated in (Nadeau et al., 2016; Acres et al., 2021). Furthermore, in the development of a microscopic system for life detection, L-serine has already been proposed to stimulate microbial motility (Lindensmith et al., 2016).

In-situ life detection instruments for the autonomous detection of motility require technical sophistication that includes classical or advanced computer vision or machine learning and needs considerable computational resources, which is challenging to accommodate for life detection missions in space (Bedrossian et al., 2018; Riekeles et al., 2021; Riekeles et al., 2024a; Wronkiewicz et al., 2024). Furthermore, the Martian sediment, which is among the most likely habitats for putative microorganisms, must be physically or (bio-)chemically separated from any hypothetical microorganisms to enhance microbial detection. To address these challenges, we suggest a simplified method (Figure 1). The methodology is based on the work of (Elgamoudi and Ketley, 2016), inducing chemotactic motility and detecting it through the usage of µ-slides and subsequent blob detection. The µ-slide devices consist of two opposing chambers separated by a semipermeable membrane, where, in principle, one of the chambers contains a chemoattractant (e.g., L-serine) and is sterile at the starting point, while the other is inoculated with putative microbes. The semipermeable membrane divides the two sections, preventing sediment particles from traversing (which we tested in a pre-experiment) and yet allowing motile organisms to pass through (i.e., traveling up the chemoattractive gradient) (Figure 2). Particles observed to have crossed the partition towards the stimulant are likely to have done so actively, indicating they are living organisms. Exploiting the principles of chemotaxis and utilizing small and relatively inexpensive µ-slides could facilitate both sediment-microbe separation, which would allow for easier imaging and computing, but, more importantly, would allow for active microbial motility detection that requires only low-computational blob detection algorithms to indicate living organisms.

We have tested the setup for the Gram-positive bacterium *B. subtilis*, the Gram-negative bacterium *P. haloplanktis*, and the archaeon *H. volcanii*. These organisms were chosen for two main reasons. Firstly, given that no extraterrestrial microbe has yet been identified, the traits necessary to survive such a harsh environment are not well understood, and, therefore, it is challenging to choose representative organisms for examination. However, we can speculate that, for survival in cold, arid, extraterrestrial climates like that of Mars, specific characteristics, such as spore-forming capacity and psychrophilic and halophilic aptitude, would likely be advantageous for survival. Each selected organism exhibits one or more of these traits, resulting in a better extraterrestrial-exemplary organism. Secondly, previous studies have found *B. subtilis* to be attracted to L-serine, allowing it to act as a positive control, and *P. haloplanktis* to be weakly repelled by L-serine, allowing us to conceptualize it as a negative control (Ordal and Gibson, 1977; Garrity and Ordal, 1995; Barbara and Mitchell, 2003). The inclusion of *H. volcanii*, a well-characterized halophilic archaeon, broadens the study's taxonomic diversity and enables insights into its chemotactic responses.

2 Materials and methods

2.1 Microorganisms used

B. subtilis, a facultative anaerobic bacterium, is one of the most extensively studied Gram-positive rod-shaped organisms. It naturally inhabits soil and is also present in the human gastrointestinal tract (van Dijl and Hecker, 2013). Due to its endospore-forming capacity, it can survive in extreme conditions, such as desiccation and temperatures up to 100°C (Nicholson et al., 2000). Typically, *B. subtilis* measures between 4 and 10 µm in length and 0.25–1 µm in diameter (Skerman et al., 1980). The bacterium is highly motile, especially during the exponential growth phase, using approximately 20 non-randomly distributed flagella per cell (Skerman et al., 1980). Depending on environmental conditions, *B. subtilis* can exhibit various forms of locomotion. One such form exhibited by *B. subtilis* is run-and-tumble motility in a biased random walk fashion, where the tumbling frequency is inversely related to the detected chemoattractant concentration (Losick, 2020). However, during the stationary phase, as the bacterium begins to form biofilms, its motility decreases, and the cells remain connected following cell division, linking to form long immobile chains in a process called chaining (Takada et al., 2014; Losick, 2020). We have used the type strain *B. subtilis* Marburg (DSM 10).

P. haloplanktis is a psychrophilic, curved rod-shaped bacterium isolated from Antarctic waters. It typically ranges from 1.2 to 2.3 µm in length and 0.5–0.6 µm in width. It is a strictly aerobic, Gram-negative, non-spore-forming, extremophile that utilizes a single polar flagellum for motility (ZoBell and Upham, 1944). Its optimal growth temperature is 20°C (Wilmes et al., 2010), yet it has the ability to grow at temperatures between −2.5°C and 29 °C (Toll-Riera et al., 2022). Given its aptitude for cold environments, we employed the type strain *P. haloplanktis* 545 (DSM 6060) in our studies.

H. volcanii, a halophilic, facultative anaerobic, mesophile, is among the most extensively studied archaea globally, primarily due to its relative ease of cultivation when compared with other archaea. Its shape varies significantly with the environment and even from cell to cell but frequently manifests itself in liquid culture as a rod

10.3389/fspas.2024.1490090

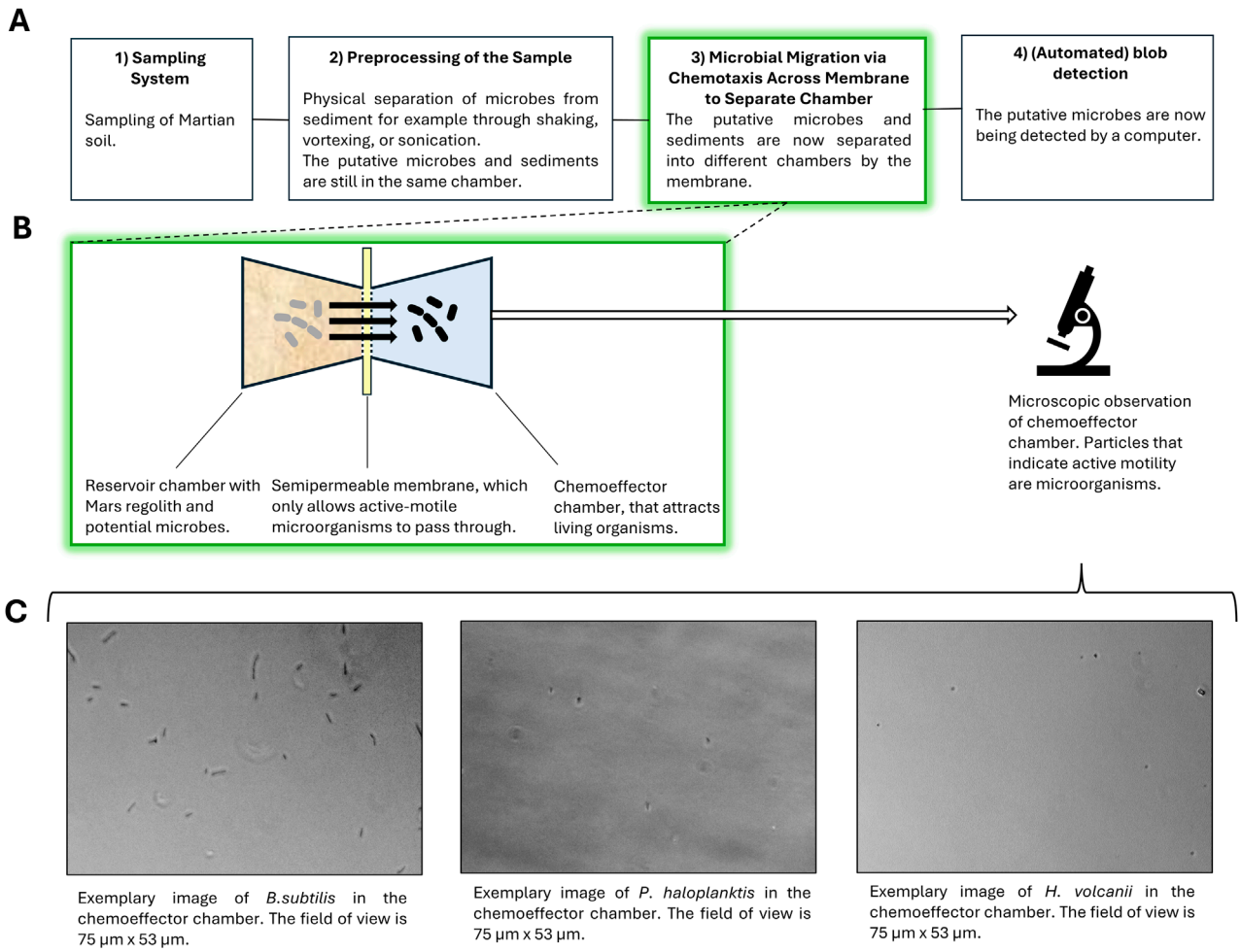

FIGURE 1
(A) Simplified workflow of the suggested life detection system. The proposed system would include 1) a sampling unit, employed for the collection of Martian soil samples; 2) a pre-processing unit, utilized for the separation of potential cells "bound" to the sediments; 3) a chemotaxis separation unit, employed for the separation of cells from the sediment containing medium; and 4) an automated processing unit for the analysis of the results in the chemotaxis separation system (i.e., blob detection). **(B)** The focus of the present work is on the chemotaxis separation system. The schematic shows a simplified structure of one of the two-chamber compartments within the µ-slide chemotaxis systems utilized for testing. A semipermeable membrane in these compartments separates the unbound cells from the original liquid medium, as the cells are attracted towards a specific chemoattractant (e.g., L-serine). Microscopic images were collected and analyzed through manual blob detection. **(C)** Three different microbes were used for testing: *B. subtilis*, *P. haloplanktis, and H. volcanii*. Exemplary microscopic images of each organism in the chemoeffector chamber are provided.

with a length of 1–3 µm and a width of 2–3 µm (Mullakhanbhai and Larsen, 1975; Chimileski et al., 2014). It holds significant interest not only for astrobiologists but also for biotechnologists due to its extensive enzymatic applications (Haque et al., 2020). Its natural habitats, including the Dead Sea, salt pans, and oceans, require it to adapt to and tolerate highly saline environments, ranging from 0.7 M to up to 2.5 M NaCl under laboratory conditions (Jantzer et al., 2011). This experiment adjusted the NaCl medium concentration to 1.7 M, which had previously been determined to be a suitable salinity for growth (Gries et al., 2022). In *H. volcanii*, motility is limited and closely associated with its pleomorphism, occurring primarily during the early exponential growth phase when the cells are more rod-shaped, before transitioning to a less motile disk shape later in their growth. The previously described archaellum-based swimming motility is the only presently known form of archaeal motility and, therefore, the means of motion employed by *H. volcanii* in this study (Kinosita et al., 2020). We have used the *H. volcanii* DS2 (DSM 3757) strain.

All strains were acquired from the Leibniz Institute DSMZ-German Collection of Microorganisms and Cell Cultures GmbH (Braunschweig, Germany).

All used organisms were isolated from previously existing stock cultures by inoculating 1 mL of this culture into sterilized 15 mL falcon tubes filled with 10 mL of the appropriate liquid media.

2.2 µ-slide experiment preparation

The necessary incubation duration prior to µ-slide experimentation was determined via a two-step inoculation process, where the first step aimed towards achieving a sufficient cell density and the second focused on deriving optimal motility. For the first

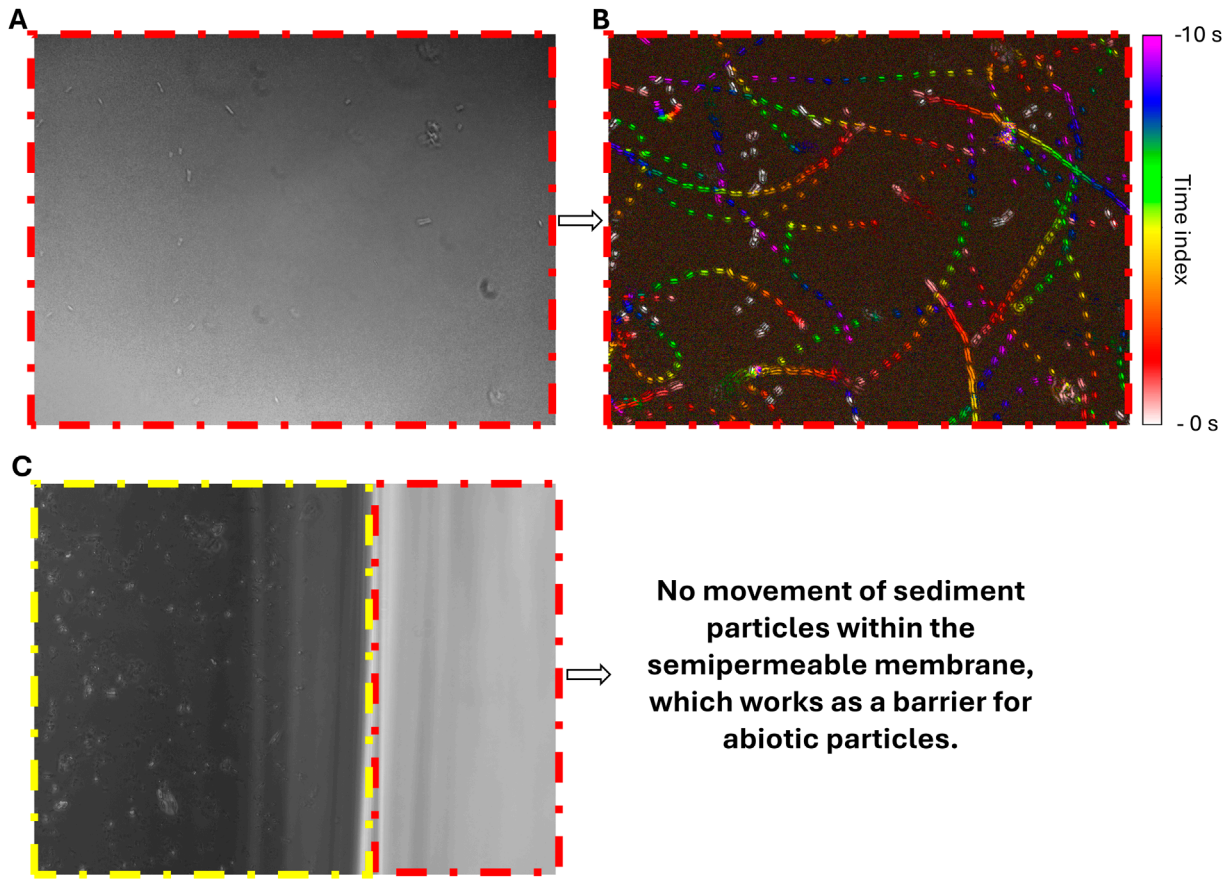

FIGURE 2
Microscopic images of the μ-slide. The red dashed boxes indicate the area of the semipermeable membrane. The yellow dashed box indicates the area of the reservoir chamber with quartz particles. All images' field of view are 141 μm × 106 μm. **(A)** Image of *B. subtilis* in semipermeable membrane. **(B)** Motion History Image (MHI) of this observation in the semipermeable membrane, indicating the microbial movement over 10 seconds. **(C)** Exemplary image of the reservoir chamber with micron-sized quartz sediments (yellow dashed box) and semipermeable membrane (red dashed box), which serves as a barrier for the sediment and shows no infiltration of sediment particles.

inoculation step, 20 μL of *B. subtilis* stock was inoculated into 2.5 mL of standard nutrient broth 1 (S1) medium (Carl Roth, Karlsruhe, Germany) and grown aerobically at 35°C for 24 h under continual shaking conditions (60 rpm). 40 μL of *P. haloplanktis* stock was grown in 2.5 mL of marine broth (MB) medium (Carl Roth, Karlsruhe, Germany) for 8 h aerobically at 25°C without shaking. 40 μL of *H. volcanii* stock was grown in '#97 low salinity' medium (composition provided in the Supplementary Material) aerobically for 48 h at 35 °C under continual shaking conditions (60 rpm). This medium was adapted from the DSMZ #97 Halobacterium medium, though the NaCl supplementation was reduced from 4.2 M to 1.7 M (further information can be found in the Supplementary Material). Thereafter, each organism's cell density was proven to be sufficient via direct microscopic observation.

Afterward, to achieve motility, each organism's respective inoculation process was repeated a second time under the same conditions and left to grow for different durations. Based on the results of (Nishihara and Freese, 1975), *B. subtilis* was anticipated to reach its desired motility state following 2–4 h of incubation. This timespan was verified through a 2 h pre-experiment that assessed the fraction of motile cells every 30 min, through the implementation of the procedure described in (Riekeles et al., 2024b). For *P. haloplanktis*, the incubation interval was set to 47–48 h 30 min, based on the methodology described in (Riekeles et al., 2021). The motility of these cells was also experimentally verified by assessing the fraction of motile cells every 30 min for 4 h. In the case of *H. volcanii*, the motility of the cells was exclusively determined through a 4 h pre-experiment with observations every hour. The final incubation interval was set to 6–8 h. The results from these individual motility pre-experiments are compiled into three different plots in the Supplementary Material.

Following the second incubation step, the 2.5 mL culture-media solutions were centrifuged for 5 min at 3,000 rpm to separate the cells from the media solution. For *H. volcanii*, centrifugation was performed twice to increase the pellet size. Subsequently, the supernatant was removed, and the pellet was washed with 1 mL of phosphate-buffered saline (PBS, composition provided in the Supplementary Material). After washing, the centrifugation process was repeated, with the PBS supernatant being removed and the new pellet being resuspended in 2.5 mL of minimal medium (MM, composition provided in the Supplementary Material) that was supplemented with NaCl according to each organism's requirements

(0.1 M for *B. subtilis,* 0.5 M for *P. haloplanktis*, and 1.7 M for *H. volcanii*). These NaCl concentrations in the MM matched those in the PBS solvent and in the original growth media, minimizing the need for the organisms to adapt osmotically. Subsequently, the samples were incubated for 1 h to acclimate to the new medium (habituation period). Following the washing procedure and acclimatization time, all organisms were shown to have maintained their viability and motility.

2.3 µ-slide experiments

The methodology for the µ-slide experiments, conducted with µ-slides chemotaxis (ibidi GmbH, Gräfelfing, Germany), is shown in Figure 3. During the habituation period, swim-agar plates were prepared. The central semipermeable membrane was developed out of MM and varying concentrations of agar-agar (Carl Roth, Karlsruhe, Germany), as tailored to the motility characteristics of each organism in an effort to approximate a standardized resistive membrane for all three organisms. Based on pre-experimental trials, agar concentrations of 0.4%, 0.3%, and 0.125% were set for *P. haloplanktis*, *B. subtilis*, and *H. volcanii*, respectively. The agar MM-agar solution was heated for 60 min in an autoclave. For each trial, 6 µL of the corresponding solution was pipetted into the central channel of each µ-slide and allowed to cool at room temperature for at least 10 min in order to set into the desired semipermeable membrane density, which ranged from a solid membrane at 0.4% to a still viscous yet more fluid liquid-like membrane at 0.125%. The right chamber of the µ-slides, designated as the chemoattractant chamber, was filled with 65 µL of liquid MM that also contained varying concentrations (0 mM, 10 mM, and 20 mM) of L-serine (AppliChem GmbH, Darmstadt, Germany), where the control (0 mM) was referenced against the two experimental concentrations (10 and 20 mM). Information on the µ-slide structure and required pipetting materials and techniques can be found in (ibidi GmbH, 2015; ibidi GmbH, 2019). Thereafter, 65 µL of each organism, suspended in their appropriate liquid MM, were added to the left chamber. The µ-slide was then covered with a lid and incubated at the original temperatures as described in Section 2.3 for 1 hour to allow the gradient to form and the organisms to migrate. All organisms, including those previously grown under shaking conditions, were returned to their appropriate incubator but left off the shaker to minimize unintended convection. The chambers were observed after 1 hour and after 3 hours. After this first incubation period of 1 hour, the filling ports were sealed with nail polish to allow for inversion of the µ-slide for microscopic analysis. Once the nail polish had dried, which took less than 5 min, the chemoattractant chamber was examined under a Primo Star Full Köhler phase contrast microscope (ZEISS, Oberkochen, Germany) utilizing the ×40 objective, which was sufficient for observation of all tested microbes. Connected to the microscope was a ZEISS Axiocam 105 color camera (ZEISS, Oberkochen, Germany) that captured 10 different images along the central region of each chemoattractant chamber at the uppermost cell-bearing focal plane to ensure consistency and reproducibility of the results. The section in the chamber captured by each of the 10 images was methodologically selected by moving in a grid-wise fashion from top to bottom before shifting to the right or left to ensure that all images were independent and had no overlap so that no cell was counted twice. The images were visualized and saved using the ZEISS ZEN 2 lite software (ZEISS, Oberkochen, Germany). The µ-slides were then returned to the incubator for another 2 hours to allow for further migration before they were subsequently observed under the microscope at the 3 hour final time point. These experiments were performed with biological triplicates.

2.4 Assessing microbial growth with L-serine

To control for the effect of microbial growth versus chemotaxis, we conducted experiments to assess whether the observed increase in cell numbers in the chemoattractors chambers was attributable to growth rather than chemotaxis. For this, we followed the preparation described in 2.2 and 2.3. After washing and a 1-h acclimatization, we put the three species separately in 10 mM and 20 mM solutions (with the corresponding NaCl concentration). For *B. subitilis*, triplicates of a control sample without serine, as well as 10 mM and 20 mM treatments, were plated immediately, 1 hour, 2 hours, and 3 hours after preparation. For *P. haloplanktis* and *H. volcanii*, OD_{600} measurements were performed in triplicate for both the control and serine-treated samples at the same time points.

2.5 Data analysis

The obtained images from the chemoattractant chambers, which had the overall dimensions of 141 µm × 106 µm, were further analyzed using the 'multi-point' tool in the Fiji (ImageJ) software for cell counting (Schindelin et al., 2012). In total, for each sample observed at each time point, including controls, 30 images were analyzed (10 for each biological triplicate). The average number of cell counts for each sample was calculated from these images. The standard deviation and standard error were also obtained for each average values (formulas provided in the Supplementary Material). All of these operations were performed with Microsoft Excel. The average cell counts of the L-serine samples were also normalized to the averages of their corresponding control samples (i.e., observed at the same time point), which resulted in a percentage of cell counts relative to the control. For further statistical analysis, the *p*-values were computed between multiple different samples, based on the Kruskal–Wallis H Test (formulas provided in the Supplementary Material). This type of statistical test was deemed more appropriate based on the distribution of the data analyzed (i.e., non-normal distribution). The *p*-values were computed with a Python script. We implemented the scripts using ChatGPT and Perplexity (November 2024 versions). The script is available in the Supplementary Material.

3 Results

3.1 *B. subtilis*

The results for *B. subtilis* growing in MM supplemented with NaCl and L-serine (in Figure 4) show that accumulated cell density

10.3389/fspas.2024.1490090

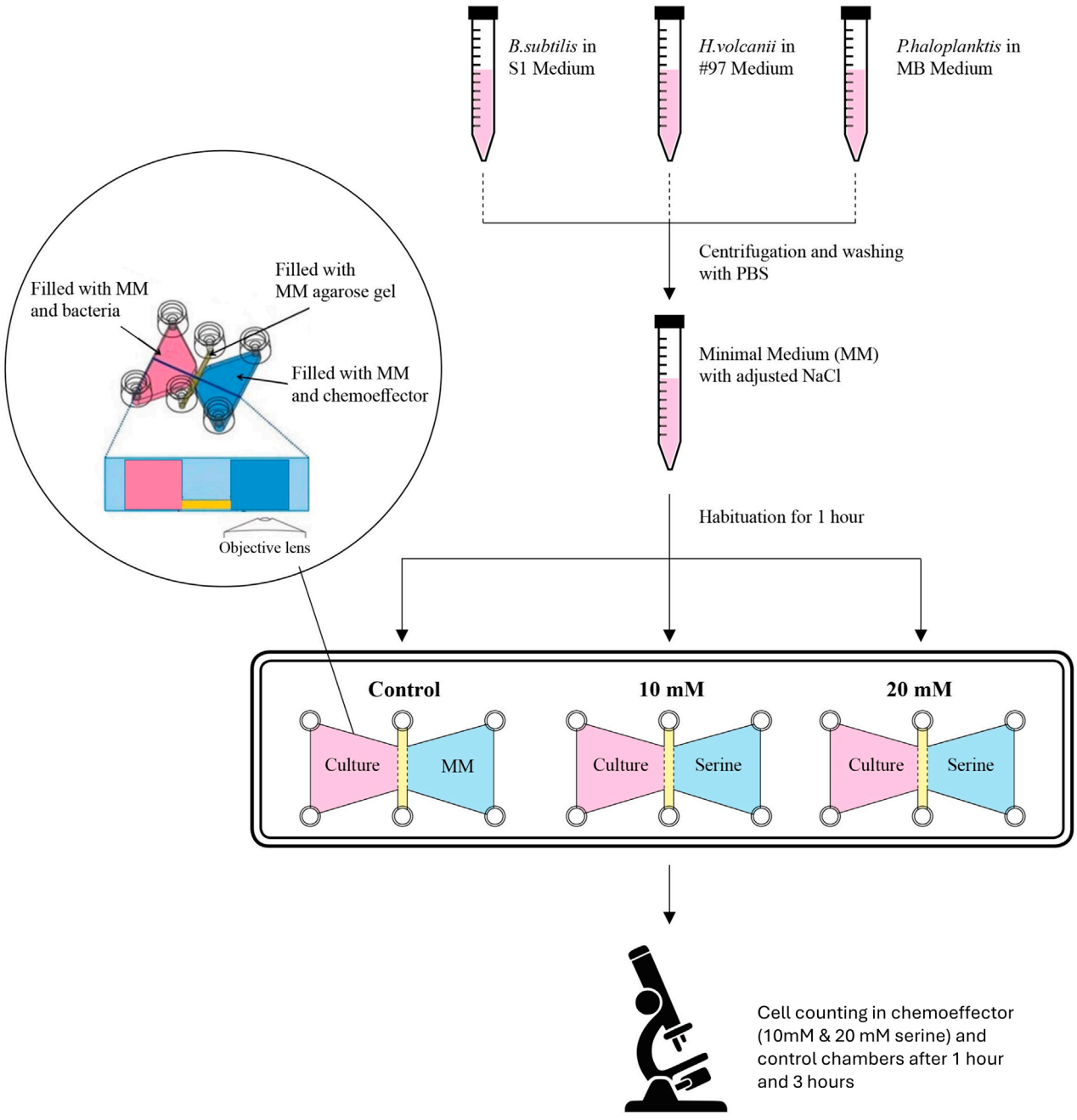

FIGURE 3
Experimental workflow of the micro-slide experiments. Each microbe used was cultivated in its own medium: S1 medium for *B. subtilis*, MB medium for *P. haloplanktis*, and #97 medium for *H. volcanii*. Before each μ-slide experiment, the cells were centrifuged, washed with PBS, and resuspended in MM supplemented with NaCl (supplementation was different for each species). The cells were allowed to habituate for 1 h in the MM, after which they were added to the respective chamber within the μ-slide. Three chambers were filled with cells for each experiment. The chemoeffector chambers were filled with MM supplemented with NaCl (control) or with NaCl + L-serine (10 mM and 20 mM). Each pair of cell/chemoeffector chambers was separated by a semipermeable membrane made-up of MM with various agarose concentrations. Observations were performed 1 h and 3 h following the completion of the μ-slide setup. 10 images were recorded for each chemoeffector chamber and biological triplicates were employed (i.e., three separate μ-slides). The experiments with each one of the three microbes were performed separately. Modified from Figure 1 in (Elgamoudi and Ketley, 2016).

within the chemoattractant chamber cannot be attributed to cell growth. Moreover, it appears that for *B. subtilis*, both 10 mM and 20 mM of L-serine contributed to a statistically significant or trending towards a significantly diminished degree of growth when compared with the control (the *p*-values are provided in the Supplementary Material).

The percentage of cell counts relative to control for *B. subtilis* are plotted in Figure 5 and provided in Table 1. *B. subtilis* displayed

10.3389/fspas.2024.1490090

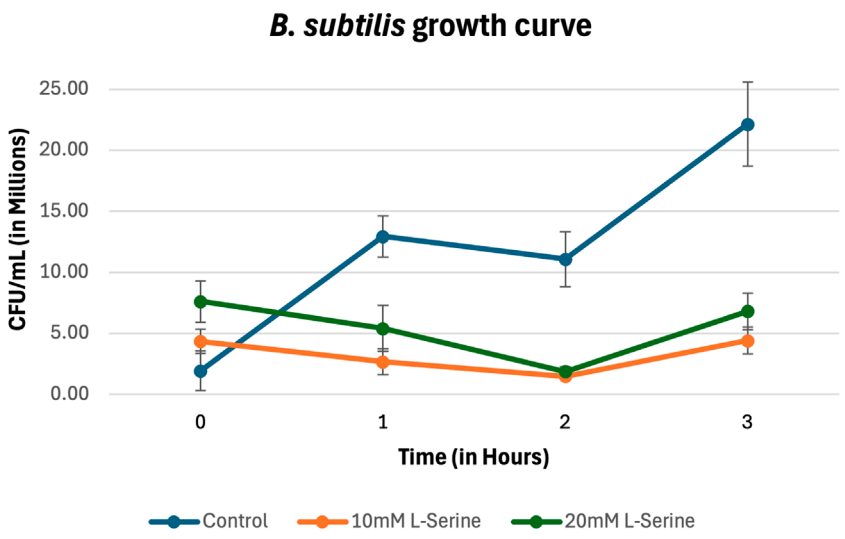

FIGURE 4
Growth curve for *B. subtilis* in MM supplemented with NaCl and L-serine across the 3-hour time period measured via plating, cell counting, and subsequent conversion into CFU/mL. The data presented consists of the average values measured from biological triplicates, with standard errors of the mean represented as error bars.

a rapid chemotactic response to the L-serine gradient resulting in a roughly 200% and 450% increase in cell density at the 1-hour timepoint within the 10 mM and 20 mM chemoattractant chambers as compared to the control cell densities at the same time point. Both values were found to be statistically significant (p-value = 1.16×10^{-4}) and (p-value = 3.68×10^{-6}), respectively. With respect to the 3-hour time point, chemoattractant chamber cell density was found to be roughly 200% and 300% greater than the control cell densities at the same time point. Once again, these values were found to be significant (p-value = 1.80×10^{-3}) and (p-value = 8.24×10^{-4}), respectively. Moreover, it should be mentioned that a statistically significant difference in cell density was found between the 10 mM and 20 mM L-serine chemoattractant chambers after 1 h, where the 20 mM chamber was nearly 225% more dense (p-value = 1.84×10^{-2}). Alternatively, such statistical significance was not maintained at the 3-h time-point, where the 20 mM chamber was roughly 50% more dense than the 10 mM L-serine chamber (p-value = 0.10). A comprehensive overview of all obtained p-values is provided in the Supplementary Material.

3.2 *P. Haloplanktis*

The results for *P. haloplanktis* growing in MM supplemented with NaCl and L-serine (Figure 6) show that accumulated cell density within the chemoattractant chamber cannot be attributed to cell growth, showing no statistically significant differences between the serine samples and the control (the p-values are provided in the Supplementary Material).

The percentage of cell counts relative to control for *P. haloplanktis* are plotted in Figure 7 and provided in Table 2. Its cell density after 1 h within the 10 mM and 20 mM L-serine chemoattractant chambers was approximately 230% and 200% greater than that of the control at the same time point. These values were deemed significant (p-value = 3.00×10^{-6}) and (p-value = 2.00×10^{-4}). No significant difference was found between the 10 mM and 20 mM cell densities at this time point (p-value = 0.11). Regarding the 3-h time-point, trends in the 10 mM and 20 mM L-serine concentrations diverged with cell density of the 20 mM chamber reaching nearly 300% of the control whereas the 10 mM chamber cell density fell to just below 150%. Though both values were found to be significantly greater than the control at the same time-point, (p-value = 6.97×10^{-4}) and (p-value = 4.90×10^{-7}), it is worth noting that a significant difference was also found to exist between the 10 mM and 20 mM cell densities at this time-point (p-value = 3.83×10^{-4}). Expanding upon this result for the 10 mM L-serine concentration, the apparent 35% decrease in cell density across the 1-to-3-hour timeframe was also statistically significant (p-value = 4.38×10^{-3}). Alternatively, the 20 mM experienced a 40% increase in cell density, which was also found to be significant (p-value = 1.79×10^{-2}). A comprehensive overview of all obtained p-values is provided in the Supplementary Material.

3.3 *H. volcanii*

Also, the results for *H. volcanii* growing in MM supplemented with NaCl and L-serine (Figure 8) show that accumulated cell density within the chemoattractant chamber cannot be attributed to cell growth, showing no statistically significant differences between the serine samples and the control (the p-values are provided in the Supplementary Material).

The percentage of cell counts relative to control for *H. volcanii* are plotted in Figure 9 and provided in Table 3. *H. volcanii* exhibited a nearly 200% increase in chemoattractant cell density following 1 h under both the 10 and 20 mM L-serine conditions with respect to the control at the same time-point. These values were significant (p-value = 5.33×10^{-3}) and (p-value = 2.01×10^{-2}). At the

10.3389/fspas.2024.1490090

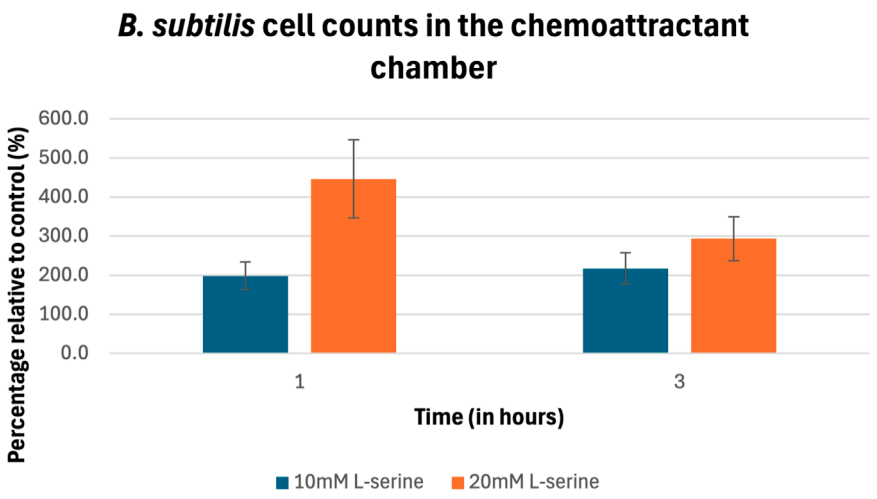

FIGURE 5
Percentage of cell counts in the 10 mM and 20 mM L-serine chemoeffector chambers relative to control for *B. subtilis* after 1 h and 3 h. The data presented consists of the average values measured from biological triplicates (n = 30), with standard errors of the mean represented as error bars.

TABLE 1 *B. subtilis* blob counts data from the 30 obtained images presented as a percentage of the control mean at the same time point (standard error).

L-serine concentration:	1 h	3 h
10 mM	198.5% (± 35.7)	217.7% (± 40.0)
20 mM	446.5% (± 100.3)	293.9% (± 56.3)

3-h timepoint, the 20 mM cell density had climbed to roughly 300% that of the control whereas the 10 mM cell density remained approximately the same. Once again, both values were found to be significantly different than the control (p-value = 5.89×10^{-4}) and (p-value = 3.74×10^{-6}), respectively. Similar to the other organisms, there was no significant difference between the 10 mM and 20 mM concentrations after 1 h of exposure, but following 3 h of exposure, the two concentrations deviated significantly, with the 20 mM concentration displaying a 160% greater cell density (p-value = 0.77 and p-value = 3.25×10^{-2}). Furthermore, it should be noted that cell density significantly increased in the 20 mM chemoattractant chamber across the 1-to-3-h transition by 155% (p-value = 1.87×10^{-2}). A comprehensive overview of all obtained p-values is provided in the Supplementary Material.

4 Discussion

The results show that all three organisms demonstrated significant chemotactic behavior in response to L-serine, further supporting the basis of chemotaxis and, more broadly, motility as an important microbial biosignature. That said, each organism's particular chemotactic response varied with respect to L-serine concentration and time of exposure. As expected, B. subtilis' chemotactic response to L-serine, which had been previously firmly established allowing it to act as a positive control (Ordal and Gibson, 1977; Garrity and Ordal, 1995), was reaffirmed across all tested concentrations and time points. The response was significant across both the 10 mM and 20 mM concentrations at the 1-hour timepoint, though it was particularly strong under the 20 mM conditions, suggesting that, at this time, higher concentrations of attractant translated to a greater chemotactic response. Interestingly, as time progressed from 1 to 3 h, there was an apparent decrease in affinity for the 20 mM concentration and no change in the affinity for the 10 mM concentration. Though the mean number of blob counts within the 10 mM and 20 mM chemoattractant chambers was greater at the 3-hour time point than the 1-hour by 360% and 215%, respectively, it should be noted that the control chamber cell density also experienced a 325% increase in cell density. This was an isolated event not observed in either of the other organism's control chambers, which remained constant throughout the experiments, suggesting that the control sample of *B. subtilis* motility increases between the 1 h and 3 h timepoint. This might be a survival mechanism due to nutrient depletion, which has also been observed for *E. coli* bacteria grown in media with a single carbon source of low-nutritional value (Ni et al., 2020).

Surprisingly, *P. haloplanktis*, which was expected to act as a negative control based on a previous study describing a repulsive effect between the microbe and L-serine (Barbara and Mitchell, 2003), also exhibited a statistically significant attractive chemotactic response to both the 10 mM and 20 mM L-serine concentrations at all observed time points. However, given that the prior studies had observed the repulsive effect at significantly lower L-serine concentrations (0.6 mM) and duration of exposure (less than 1 min), these findings do not directly contradict the earlier study (Barbara and Mitchell, 2003). A biphasic response has been observed in E. coli when leucine is used as a signaling molecule and was either an attractant or repellent, depending on its concentration (Khan and Trentham, 2004). *P. haloplanktis* might exhibit a similar response when exposed to L-serine. This highlights the importance of revisiting and reassessing established biological understandings,

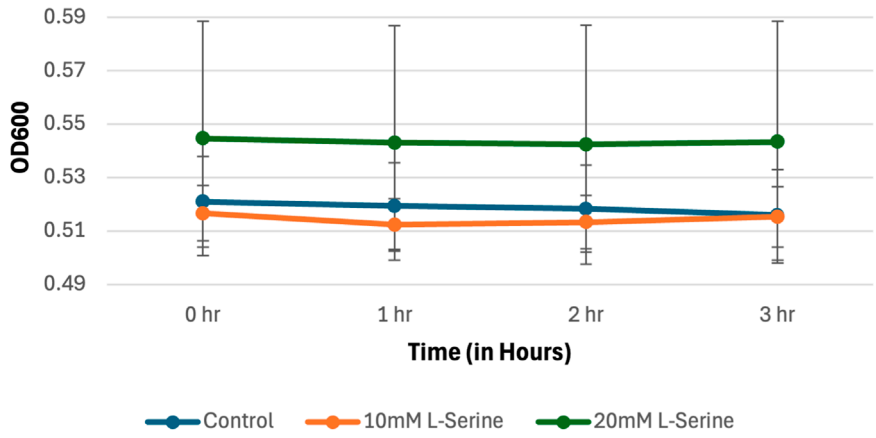

FIGURE 6
Growth curve for *P. haloplanktis* in MM supplemented with NaCl and L-serine across the 3-hour time period measured via plating, cell counting, and subsequent conversion into CFU/mL. The data presented consists of the average values measured from biological triplicates, with standard errors of the mean represented as error bars.

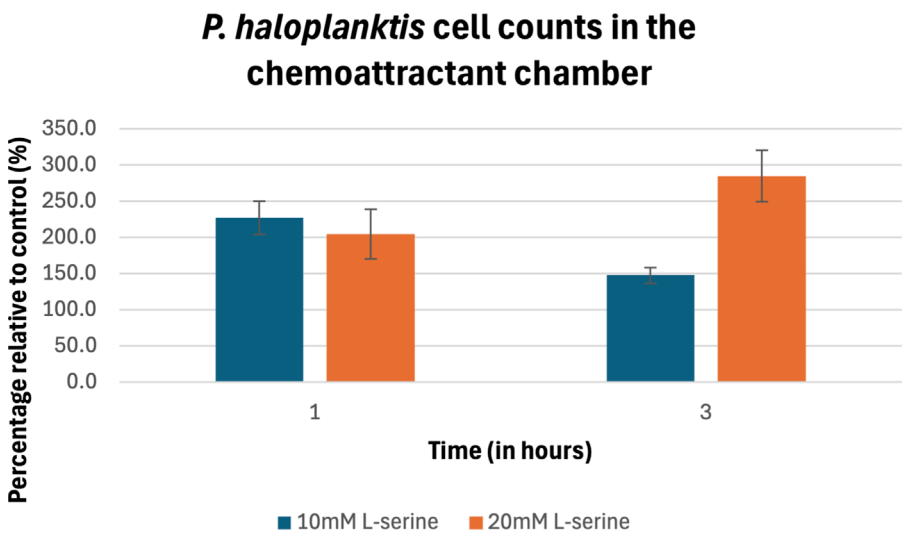

FIGURE 7
Percentage of cell counts in the 10 mM and 20 mM L-serine chemoeffector chambers relative to control for *P. haloplanktis* after 1 h and 3 h. The data presented consists of the average values measured from biological triplicates (n = 30), with standard errors of the mean represented as error bars.

TABLE 2 *P. haloplanktis* blob counts data from the 30 obtained images presented as a percentage of the control mean at the same time point (standard error).

L-serine concentration:	1 h	3 h
10 mM	227.1% (± 23.1)	147.3% (± 11.0)
20 mM	204.3% (± 34.2)	284.4% (± 35.4)

especially under different experimental conditions or environmental contexts, as a particular chemoattractant's repulsive or attractive nature can vary with concentration, duration of exposure, and likely other situational factors. Moreover, the transition from 1 to 3 h was a point of interest as the results diverged for the 10 mM and 20mM, where, despite the 20 mM cell density deviating insignificantly from the 1-hour timepoint, the 10 mM chamber cell density was significantly less than both its 1-hour density and the 3-h 20 mM cell density. Synthesizing these results with the previously reported study, it appears that *P. haloplanktis*' chemotactic response towards L-serine can be conceptualized as a scaled transition from repulsive at lower chemotactic agent concentrations and durations, such as 0.6 mM and less than a minute, towards attractive at higher concentrations and longer durations of exposure, such as 20 mM at 1 h. The caveat being, however, that intermediary concentrations still

10.3389/fspas.2024.1490090

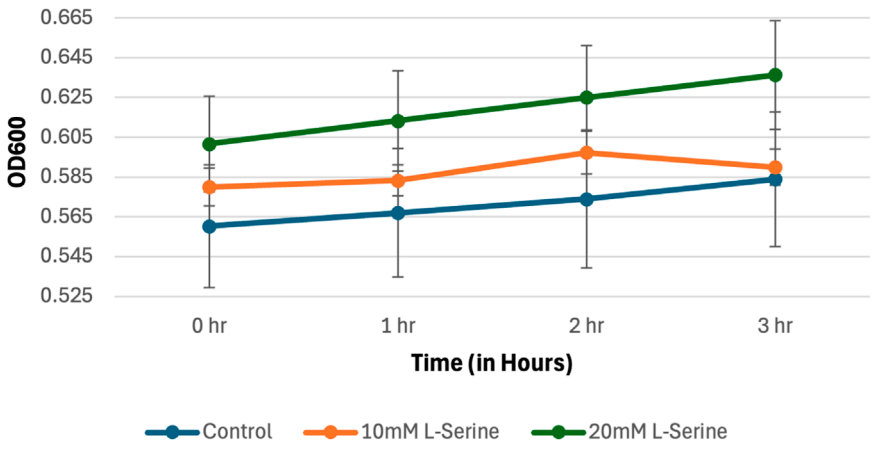

FIGURE 8
Growth curve for *H. volcanii* in MM supplemented with NaCl and L-serine across the 3-hour time period measured via plating, cell counting, and subsequent conversion into CFU/mL. The data presented consists of the average values measured from biological triplicates, with standard errors of the mean represented as error bars.

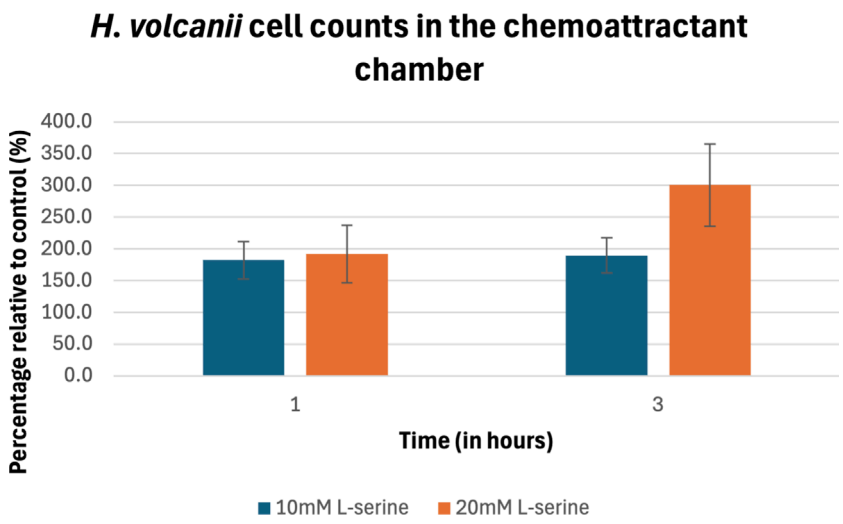

FIGURE 9
Percentage of cell counts in the 10 mM and 20 mM L-serine chemoeffector chambers relative to control for *H. volcanii* after 1 h and 3 h. The data presented consists of the average values measured from biological triplicates (n = 30), with standard errors of the mean represented as error bars.

TABLE 3 *H. volcanii* blob counts data from the 30 obtained images presented as a percentage of the control mean at the same time point (standard error).

L-serine concentration:	1 h	3 h
10 mM	182.0% (± 29.4)	189.6% (± 27.7)
20 mM	192.2% (± 45.5)	300.5% (± 64.6)

capable of inducing a significant attractive response, such as 10 mM, trend more quickly towards being weaker, indifferent, or possibly even repulsive stimuli as time progresses and the attractant gradient disperses than higher concentrations, such as 20 mM, which were able to maintain their affinity across the 3-h time period. Further work will be needed to address the concentrations and durations of exposure at which there is a transition in the chemotactic response from repulsive to attractive and *vice versa*.

Research on the chemotactic behavior of archaea has been relatively limited until recent years. However, a growing focus on *H. volcanii* within the scientific community has significantly deepened our understanding (Kokoeva et al., 2002; Quax et al., 2018; Li et al., 2019). The question of whether L-serine induces chemotaxis in H. volcanii had not been addressed before this study. The results presented here suggest, for the first time, an increased attraction of

the archaeon toward both the 10 mM and 20 mM concentrations of L-serine. When observed after 1 h, there was no apparent difference in the microbe's affinity for the differing chemoattractant concentrations. However, after 3 h there was a significant contrast in chemotactic responses between the two concentrations with an increasing affinity for the higher concentration whereas the affinity for the 10 mM remained approximately the same throughout the study together suggesting that as time progresses *H. volcanii*'s chemotactic response towards higher concentrations, such as 20 mM, becomes more attractive. In contrast, the response towards lower concentrations, such as 10 mM, remains relatively constant.

With respect to the presented results for all three organisms, it should be noted that observed increases in chemoattractant chamber cell density across the 3-h time period were attributed to a flux of individual microbes chemotactically traversing the semipermeable-membrane up the L-serine gradient rather than cells metabolically utilizing L-serine as a carbon source permitting cell growth beyond what would normally be feasible within the provided minimal medium. This conclusion was supported by growth curves for all three organisms across the entirety of the 3-h experiment following the PBS washing procedure.

The study's experimental setup diverged from earlier protocols, in which the μ-slides were used for long-term chemotactic assays lasting up to 24 h (Elgamoudi and Ketley, 2016). Previous methodologies generally filled both distal chambers of the μ-slide with a concentration of agarose gel up to 1% (Elgamoudi and Ketley, 2016). Alternatively, this experiment focused efforts on a much shorter duration for chemotactic observation by electing to remove the motile-resistive agarose in both the right chemoattractant chamber as well as in the left organismal chamber, effectively restricting the presence of agarose to only the central semipermeable membrane. This modification allows for less resistive movement within each chamber, yet still retains the capacity for interchamber selective permeability. The approach proved viable and can be utilized in the future as a more time-effective alternative for studies of microbial motility, such as on *in-situ* life detection missions in which longer-duration cultivation may not be possible. Like in previous space-related research (Lindensmith et al., 2016), the use of L-serine in these experiments proved successful, justifying further investigation.

As with any other technique intended to investigate the existence of extraterrestrial life, methodological assumptions must be made and addressed as limitations of the approach to specifying the approach's breadth of utility. Three such limiting assumptions made in this study are 1) that extraterrestrial life would have the capacity for chemotaxis, in this case in response to L-serine at a particular concentration and time point, and 2) that not only is the semipermeable membrane capable of resisting non-cellular interchamber translocation of sediment particles at various agar concentrations but also that 3) researchers have prior knowledge of the desired isolated organism's motility characteristics so as to properly adjust the membrane's density. At present, these assumptions are likely too restrictive for this approach to be put into practice during life detection missions on Mars or other planetary bodies, where such prior knowledge is unknown.

Further studies could address these limitations and, thereby, make this approach more practical by incorporating a more comprehensive variety of chemoattractants including other amino acids or glucose, which, despite L-serine's chemotactic potency across all three domains of known life, would provide an even more extensive chemotactic stimulus reaching organisms that would not otherwise be chemotactically sensitive. As previously stated, organic compounds with biological relevance, such as racemic mixtures of various proteinogenic and non-proteinogenic amino acids, have been found in extraterrestrial samples such as the Murchison meteorite and asteroid (162173) Ryugu (Koga and Naraoka, 2017; Naraoka et al., 2023). Moreover, there is evidence suggesting the existence of ribose and other essential sugars within primitive meteorites (Furukawa et al., 2019). On Earth, many of these detected molecules have demonstrated the ability to induce chemotactic responses in species including *E. coli's* sensitivity towards ribose, L-alanine, and various other amino acids and *B. subtilis*' response to glycine and cysteine, amongst other stimulants (Ordal and Gibson, 1977; Kondoh et al., 1979; Yang et al., 2015). Given their existence in space and capacity for chemotactic stimulation, the methodology presented here could be adapted to include these attractants individually or in unique combinations in an effort to induce a greater response magnitude and a broader spectrum of reactivity. In future studies, the limitations of the semipermeable membrane should be further addressed through the development of an agnostic semipermeable membrane; meaning a membrane that maintains its ability to restrict noncellular translocation yet also, without additional density manipulation, permits the passage of a broader spectrum of potential microbes with various sizes, shapes, and biochemical properties.

5 Conclusion

Chemotaxis remains a broad and only partially understood field that holds much promise for both living microbe isolation and identification that would be of interest to a variety of disciplines. In the context of astrobiology, ongoing research is required to facilitate the most resource-effective methodology that could be used for *in-situ* life detection missions. When synthesized with previous findings, this study's results effectively demonstrate the viability of μ-slides for chemotactic observation of prokaryotes across shorter (several hours) and longer (up to 24 h) timeframes. Though further adaptation is required for its real-life feasibility, the minimal necessary technical and resource requirements, as well as the reduced need for continuous observation, make their usage an attractive and feasible alternative for space missions, where power, operator handling, data storage, and complex data processing capabilities are limited.

Data availability statement

The original contributions presented in the study are publicly available in the DepositOnce repository at: https://doi.org/10.14279/depositonce-22339.

Author contributions

MR: Data curation, Funding acquisition, Investigation, Methodology, Software, Validation, Visualization, Writing–original draft, Writing–review and editing. VB: Data curation, Investigation, Validation, Visualization, Writing–original draft, Writing–review and editing. NA: Data curation, Methodology, Formal analysis, Validation, Investigation, Writing–review and editing. BS: Data curation, Investigation, Methodology, Software, and Formal analysis. DS-M: Conceptualization, Methodology, Resources, Supervision, Writing–original draft, Writing–review and editing.

Funding

The author(s) declare that financial support was received for the research, authorship, and/or publication of this article. This work was financially supported in part by the Friedrich Ebert Foundation.

Acknowledgments

We would like to give a special thanks to the reviewers, who through their careful consideration of the article during the editing process, brought forward insightful concerns leading to corrections that strengthened both the structure and content of the manuscript. We also would like to thank Florian Carlo Fischer for helpful feedback and conversations. Moreover, we would like to acknowledge that both AI platforms ChatGPT and Perplexity were consulted during the experimental set up for the most effective statistical analysis methodology as well as for the implementation of the statistical scripts later run on Python. These AI platforms are cited below. Perplexity AI. (2024). *Perplexity AI* (Nov 26 version) [Large language model]. https://www.perplexity.ai/ OpenAI. (2024). ChatGPT (Nov 20 version) [Large language model]. https://chat.openai.com/chat.

Conflict of interest

The authors declare that the research was conducted in the absence of any commercial or financial relationships that could be construed as a potential conflict of interest.

Publisher's note

All claims expressed in this article are solely those of the authors and do not necessarily represent those of their affiliated organizations, or those of the publisher, the editors and the reviewers. Any product that may be evaluated in this article, or claim that may be made by its manufacturer, is not guaranteed or endorsed by the publisher.

References

Acres, J. M., Youngapelian, M. J., and Nadeau, J. (2021). The influence of spaceflight and simulated microgravity on bacterial motility and chemotaxis. *NPJ Microgravity* 7, 7. doi:10.1038/s41526-021-00135-x

Aizawa, S. I. (1996). Flagellar assembly in Salmonella typhimurium. *Mol. Microbiol.* 19, 1–5. doi:10.1046/j.1365-2958.1996.344874.x

Albers, S.-V., and Jarrell, K. F. (2018). The archaellum: an update on the unique archaeal motility structure. *Trends Microbiol.* 26, 351–362. doi:10.1016/j.tim.2018.01.004

Allen, R. D. (1981). Motility. *J. cell Biol.* 91, 148s–155s. doi:10.1083/jcb.91.3.148s

BacDive (2024). BacDive dashboard. Available at: https://bacdive.dsmz.de/dashboard (Accessed August 20, 2024).

Barbara, G. M., and Mitchell, J. G. (2003). Marine bacterial organisation around point-like sources of amino acids. *FEMS Microbiol. Ecol.* 43, 99–109. doi:10.1016/s0168-6496(02)00401-4

Bardy, S. L., Ng, S. Y. M., and Jarrell, K. F. (2003). Prokaryotic motility structures. *Microbiol. Read.* 149, 295–304. doi:10.1099/mic.0.25948-0

Bedrossian, M., El-Kholy, M., Neamati, D., and Nadeau, J. (2018). A machine learning algorithm for identifying and tracking bacteria in three dimensions using Digital Holographic Microscopy. *AIMS Biophys.* 5, 36–49. doi:10.3934/biophy.2018.1.36

Braakman, R., and Smith, E. (2012). The emergence and early evolution of biological carbon-fixation. *PLoS Comput. Biol.* 8, e1002455. doi:10.1371/journal.pcbi.1002455

Chimileski, S., Franklin, M. J., and Papke, R. T. (2014). Biofilms formed by the archaeon Haloferax volcanii exhibit cellular differentiation and social motility, and facilitate horizontal gene transfer. *BMC Biol.* 12, 65. doi:10.1186/s12915-014-0065-5

Colin, R., Ni, B., Laganenka, L., and Sourjik, V. (2021). Multiple functions of flagellar motility and chemotaxis in bacterial physiology. *FEMS Microbiol. Rev.* 45, fuab038. doi:10.1093/femsre/fuab038

Craig, L., Forest, K. T., and Maier, B. (2019). Type IV pili: dynamics, biophysics and functional consequences. *Nat. Rev. Microbiol.* 17, 429–440. doi:10.1038/s41579-019-0195-4

Elgamoudi, B., and Ketley, J. (2016). *Determ. Chemotactic Behav. Campylobacter jejuni by using μ-Slide. Chemotaxis. User Protoc. 01*. Available at: https://ibidi.com/img/cms/support/UP/UP01_Elgamoudi_Chemotaxis.PDF (Accessed August 21, 2024).

Fenchel, T., and Thar, R. (2004). Candidatus Ovobacter propellens: a large conspicuous prokaryote with an unusual motility behaviour. *FEMS Microbiol. Ecol.* 48, 231–238. doi:10.1016/j.femsec.2004.01.013

Furukawa, Y., Chikaraishi, Y., Ohkouchi, N., Ogawa, N. O., Glavin, D. P., Dworkin, J. P., et al. (2019). Extraterrestrial ribose and other sugars in primitive meteorites. *Proc. Natl. Acad. Sci.* 116, 24440–24445. doi:10.1073/pnas.1907169116

Garrity, L. F., and Ordal, G. W. (1995). Chemotaxis in Bacillus subtilis: how bacteria monitor environmental signals. *Pharmacol. Ther.* 68, 87–104. doi:10.1016/0163-7258(95)00027-5

Gries, A., Heinz, J., and Schulze-Makuch, D. (2022). "Perchlorate stress responses of Haloferax volcanii and implications on the habitability of Mars," in *Europlanet science congress 2022*. Granada, Spain.

Grossart, H. P., Riemann, L., and Azam, F. (2001). Bacterial motility in the sea and its ecological implications. *Aquat. Microb. Ecol.* 25, 247–258. doi:10.3354/ame025247

Hölscher, T., and Kovács, Á. T. (2017). Sliding on the surface: bacterial spreading without an active motor. *Environ. Microbiol. Instr. μ–Slide Chemotaxis* 19, 2537–2545. doi:10.1111/1462-2920.13741

ibidi, GmbH (2015). Instructions μ–slide chemotaxis. (Accessed November 28, 2024).620 Available at: https://ibidi.com/img/cms/products/labware/channel_slides/S_8032X_Chemotaxis/IN_8032X_Che621motaxis.pdf.

ibidi, GmbH (2019). Important handling information for the μ-slide chemotaxis. (Accessed November 28, 2024).624 Available at: https://ibidi.com/img/cms/resources/important_info/II_501_Important_Info_Chemotaxis_150dpi.p625df.

Jarrell, K. F., Albers, S.-V., and Machado, J. N. d. S. (2021). A comprehensive history of motility and Archaellation in Archaea. *FEMS Microbes* 2, xtab002. doi:10.1093/femsmc/xtab002

Khan, S., and Trentham, D. R. (2004). Biphasic excitation by leucine in *Escherichia coli* chemotaxis. *J. Bacteriol.* 186, 588–592. doi:10.1128/JB.186.2.588-592.2004

Kinosita, Y., Mikami, N., Li, Z., Braun, F., Quax, T. E. F., van der Does, C., et al. (2020). Motile ghosts of the halophilic archaeon, Haloferax volcanii. *Proc. Natl. Acad. Sci.* 117, 26766–26772. doi:10.1073/pnas.2009814117

Koga, T., and Naraoka, H. (2017). A new family of extraterrestrial amino acids in the Murchison meteorite. *Sci. Rep.* 7, 636. doi:10.1038/s41598-017-00693-9

Kokoeva, M. V., Storch, K.-F., Klein, C., and Oesterhelt, D. (2002). A novel mode of sensory transduction in archaea: binding protein-mediated chemotaxis towards osmoprotectants and amino acids. *EMBO J.* 21, 2312–2322. doi:10.1093/emboj/21.10.2312

Kondoh, H., Ball, C. B., and Adler, J. (1979). Identification of a methyl-accepting chemotaxis protein for the ribose and galactose chemoreceptors of *Escherichia coli*. *Proc. Natl. Acad. Sci. U. S. A.* 76, 260–264. doi:10.1073/pnas.76.1.260

Li, Z., Kinosita, Y., Rodriguez-Franco, M., Nußbaum, P., Braun, F., Delpech, F., et al. (2019). Positioning of the motility machinery in halophilic archaea. *mBio* 10, 1–3. doi:10.1128/mBio.00377-19

Lindensmith, C. A., Rider, S., Bedrossian, M., Wallace, J. K., Serabyn, E., Showalter, G. M., et al. (2016). A submersible, off-Axis holographic microscope for detection of microbial motility and morphology in aqueous and icy environments. *PLOS ONE* 11, e0147700. doi:10.1371/journal.pone.0147700

Losick, R. M. (2020). Bacillus subtilis: a bacterium for all seasons. *Curr. Biol.* 30, R1146–R1150. doi:10.1016/j.cub.2020.06.083

Madigan, M. T., Bender, K. S., Buckley, D. H., Sattley, W. M., and Stahl, D. A. (2018). *Brock biology of microorganisms*. Global Edition. Harlow: Pearson Education, Limited.

Mattick, J. S. (2002). Type IV pili and twitching motility. *Annu. Rev. Microbiol.* 56, 289–314. doi:10.1146/annurev.micro.56.012302.160938

Merz, A. J., So, M., and Sheetz, M. P. (2000). Pilus retraction powers bacterial twitching motility. *Nature* 407, 98–102. doi:10.1038/35024105

Mesibov, R., and Adler, J. (1972). Chemotaxis toward amino acids in Escherichia coli. *J. Bacteriol.* 112, 315–326. doi:10.1128/jb.112.1.315-326.1972

Miyata, M., Robinson, R. C., Uyeda, T. Q. P., Fukumori, Y., Fukushima, S.-I., Haruta, S., et al. (2020). Tree of motility - a proposed history of motility systems in the tree of life. *Genes cells.* 25, 6–21. doi:10.1111/gtc.12737

Mullakhanbhai, M. F., and Larsen, H. (1975). Halobacterium volcanii spec. nov., a Dead Sea halobacterium with a moderate salt requirement. *Arch. Microbiol.* 104, 207–214. doi:10.1007/BF00447326

Nadeau, J., Lindensmith, C., Deming, J. W., Fernandez, V. I., and Stocker, R. (2016). Microbial morphology and motility as biosignatures for outer planet missions. *Astrobiology* 16, 755–774. doi:10.1089/ast.2015.1376

Nadeau, J. L., Bedrossian, M., and Lindensmith, C. A. (2018). Imaging technologies and strategies for detection of extant extraterrestrial microorganisms. *Adv. Phys. X* 3, 1424032. doi:10.1080/23746149.2018.1424032

Naraoka, H., Takano, Y., Dworkin, J. P., Oba, Y., Hamase, K., Furusho, A., et al. (2023). Soluble organic molecules in samples of the carbonaceous asteroid (162173) Ryugu. *Science* 379, eabn9033. doi:10.1126/science.abn9033

Neveu, M., Hays, L. E., Voytek, M. A., New, M. H., and Schulte, M. D. (2018). The ladder of life detection. *Astrobiology* 18, 1375–1402. doi:10.1089/ast.2017.1773

Ni, B., Colin, R., Link, H., Endres, R. G., and Sourjik, V. (2020). Growth-rate dependent resource investment in bacterial motile behavior quantitatively follows potential benefit of chemotaxis. *Proc. Natl. Acad. Sci.* 117, 595–601. doi:10.1073/pnas.1910849117

Nicholson, W. L., Munakata, N., Horneck, G., Melosh, H. J., and Setlow, P. (2000). Resistance of Bacillus endospores to extreme terrestrial and extraterrestrial environments. *Microbiol. Mol. Biol. Rev.* 64, 548–572. doi:10.1128/mmbr.64.3.548-572.2000

Nishihara, T., and Freese, E. (1975). Motility of *Bacillus subtilis* during growth and sporulation. *J. Bacteriol.* 123, 366–371. doi:10.1128/jb.123.1.366-371.1975

Nuno de Sousa Machado, J., Albers, S.-V., and Daum, B. (2022). Towards elucidating the rotary mechanism of the archaellum machinery. *Front. Microbiol.* 13, 848597. doi:10.3389/fmicb.2022.848597

Ordal, G. W., and Gibson, K. J. (1977). Chemotaxis toward amino acids by Bacillus subtilis. *J. Bacteriol.* 129, 151–155. doi:10.1128/JB.129.1.151-155.1977

Oxenrider, K. A., and Kennelly, P. J. (1993). A protein-serine phosphatase from the halophilic archaeon Haloferax volcanii. *Biochem. Biophys. Res. Commun.* 194, 1330–1335. doi:10.1006/bbrc.1993.1970

Pizzarello, S., and Shock, E. (2010). The organic composition of carbonaceous meteorites: the evolutionary story ahead of biochemistry. *Cold Spring Harb. Perspect. Biol.* 2, a002105. doi:10.1101/cshperspect.a002105

Quax, T. E. F., Albers, S.-V., and Pfeiffer, F. (2018). Taxis in archaea. *Emerg. Top. Life Sci.* 2, 535–546. doi:10.1042/ETLS20180089

Reimer, L. C., Sardà Carbasse, J., Koblitz, J., Ebeling, C., Podstawka, A., and Overmann, J. (2022). BacDive in 2022: the knowledge base for standardized bacterial and archaeal data. *Nucleic Acids Res.* 50, D741–D746. doi:10.1093/nar/gkab961

Riekeles, M., Albalkhi, H., Dubay, M. M., Nadeau, J., and Lindensmith, C. A. (2024a). Motion history images: a new method for tracking microswimmers in 3D. *Front. Imaging* 3. doi:10.3389/fimag.2024.1393314

Riekeles, M., Santos, B., Youssef, S. A.-M., and Schulze-Makuch, D. (2024b). Viability and motility of *Escherichia coli* under elevated martian salt stresses. *Life (Basel)* 14, 1526. doi:10.3390/life14121526

Riekeles, M., Schirmack, J., and Schulze-Makuch, D. (2021). Machine learning algorithms applied to identify microbial species by their motility. *Life (Basel)* 11, 44. doi:10.3390/life11010044

Schindelin, J., Arganda-Carreras, I., Frise, E., Kaynig, V., Longair, M., Pietzsch, T., et al. (2012). Fiji: an open-source platform for biological-image analysis. *Nat. Methods* 9, 676–682. doi:10.1038/nmeth.2019

Skerker, J. M., and Berg, H. C. (2001). Direct observation of extension and retraction of type IV pili. *Proc. Natl. Acad. Sci. U. S. A.* 98, 6901–6904. doi:10.1073/pnas.121171698

Skerman, V., McGowan, V., and Sneath, P. (1980). Approved lists of bacterial names. *Int. J. Syst. Evol. Microbiol.* 30, 225–420. doi:10.1099/00207713-30-1-225

Soutourina, O. A., Semenova, E. A., Parfenova, V. V., Danchin, A., and Bertin, P. (2001). Control of bacterial motility by environmental factors in polarly flagellated and peritrichous bacteria isolated from Lake Baikal. *Appl. Environ. Microbiol.* 67, 3852–3859. doi:10.1128/AEM.67.9.3852-3859.2001

Takada, H., Morita, M., Shiwa, Y., Sugimoto, R., Suzuki, S., Kawamura, F., et al. (2014). Cell motility and biofilm formation in Bacillus subtilis are affected by the ribosomal proteins, S11 and S21. *Biosci. Biotechnol. Biochem.* 78, 898–907. doi:10.1080/09168451.2014.915729

Thomas-Keprta, K. L., Clemett, S. J., Bazylinski, D. A., Kirschvink, J. L., McKay, D. S., Wentworth, S. J., et al. (2002). Magnetofossils from ancient Mars: a robust biosignature in the martian meteorite ALH84001. *Appl. Environ. Microbiol.* 68, 3663–3672. doi:10.1128/AEM.68.8.3663-3672.2002

Tohidifar, P., Bodhankar, G. A., Pei, S., Cassidy, C. K., Walukiewicz, H. E., Ordal, G. W., et al. (2020). The unconventional cytoplasmic sensing mechanism for ethanol chemotaxis in Bacillus subtilis. *mBio* 11, 10–12. doi:10.1128/mBio.02177-20

Toll-Riera, M., Olombrada, M., Castro-Giner, F., and Wagner, A. (2022). A limit on the evolutionary rescue of an Antarctic bacterium from rising temperatures. *Sci. Adv.* 8, eabk3511. doi:10.1126/sciadv.abk3511

van Dijl, J. M., and Hecker, M. (2013). Bacillus subtilis: from soil bacterium to super-secreting cell factory. *Microb. Cell Factories* 12, 3. doi:10.1186/1475-2859-12-3

Vuppula, R. R., Tirumkudulu, M. S., and Venkatesh, K. V. (2010). Chemotaxis of Escherichia coli to L-serine. *Phys. Biol.* 7, 026007. doi:10.1088/1478-3975/7/2/026007

Wilmes, B., Hartung, A., Lalk, M., Liebeke, M., Schweder, T., and Neubauer, P. (2010). Fed-batch process for the psychrotolerant marine bacterium Pseudoalteromonas haloplanktis. *Microb. Cell Factories* 9, 72. doi:10.1186/1475-2859-9-72

Wronkiewicz, M., Lee, J., Mandrake, L., Lightholder, J., Doran, G., Mauceri, S., et al. (2024). Onboard science instrument autonomy for the detection of microscopy biosignatures on the ocean worlds life surveyor. *Planet. Sci. J.* 5, 19. doi:10.3847/PSJ/ad0227

Yang, Y., M Pollard, A., Höfler, C., Poschet, G., Wirtz, M., Hell, R., et al. (2015). Relation between chemotaxis and consumption of amino acids in bacteria. *Mol. Microbiol.* 96, 1272–1282. doi:10.1111/mmi.13006

Zhu, K., Schiller, M., Pan, L., Saji, N. S., Larsen, K. K., Amsellem, E., et al. (2022). Late delivery of exotic chromium to the crust of Mars by water-rich carbonaceous asteroids. *Sci. Adv.* 8, eabp8415. doi:10.1126/sciadv.abp8415

ZoBell, C. E., and Upham, H. C. (1944). *A list of marine bacteria including descriptions of sixty new species*. Berkeley: University of California Press.